Reversible Amorphous-to-Amorphous Transitions in Chalcogenide Films: Correlating Changes in Structure and Optical Properties

Maria Kalyva, Jiri Orava, Angeliki Siokou, Martin Pavlista, Tomas Wagner, and Spyros N. Yannopoulos**

Structural transitions in materials are accompanied by appreciable and exploitable changes in physical-chemical properties. Whereas reversible optically-driven atomistic changes in crystal-to-amorphous transitions are generally known and exploited in applications, the nature of the corresponding polyamorphic transitions between two structurally distinct meta-stable amorphous phases is an unexplored theme. Direct experimental evidence is reported for the nature of the atomistic changes during fully reversible amorphous-to-amorphous switching between two individual states in the non-crystalline $As_{50}Se_{50}$ films prepared by pulsed-laser deposition and consequent changes in optical properties. Combination of surface sensitive X-ray photoelectron spectroscopy and spectroscopic ellipsometry show that the near-bandgap energy illumination and annealing induce reversible switching in the material's structure by local bonding rearrangements. This is accompanied by switching in refractive index between two well-defined states. Exploiting the pluralism of distinct structural states in a disordered solid can provide new insights into the data storage in emerging optical memory and photonic applications.

1. Introduction

Over the last few decades we have witnessed a tremendous upsurge of interest in chalcogenide glasses (ChGs) and their potential applications as photonic glasses (for example, all optical switching devices).[1] Passive and active applications of ChGs are based on (i) the enhanced infrared light transmittance without changing the optical properties of the glass, and (ii) the interaction between the transmitted light and the glass through nonlinear effects (both second- and third-order).[2] It has been demonstrated that the photonic bandgap in certain materials can be tuned by using, for example, external pressure or bias,[3,4] and that such dependence of the photonic bandgap on pressure can be exploited in sensitive pressure sensors. The shift in photonic bandgap can also be caused by having two distinct meta-stable structural states in the glass with considerably different optical properties, namely the refractive index (n). In addition, certain chalcogenides exhibit a reversible phase-change (PC) amorphous-to-crystal transition under the influence of external stimuli and therefore have been used in low-power and fast data storage applications. Electric current (Joule heating) is such a stimulus, the role of which in switching had been demonstrated long ago by Ovshinsky[5] and is the principal operation of nonvolatile PC random-access memory (PC-RAM). Alternatively, heating can be induced by visible, above-bandgap light, which leads to optically-induced PC[6] used in optical recording: CD-RW (compact disc - rewritable), DVD±RW (digital versatile disc - rewritable) and Blu-Ray disc. The key idea is that local structural differences in PC memory are manifested through measurable lower conductivity and reflectance of the amorphous phase contrary to the crystalline state. Various compositions of the ternary Ge-Sb-Te alloy are undoubtedly today the best-known PC materials. Numerous experimental and simulation studies have focused on explaining the structural changes responsible for the fast (< 100 ns, and preferably faster) PC at the atomic level.[7–11]

Up until now, the vast majority of studies in the quest for optical recording have been devoted to PC transitions. On the

Dr. M. Kalyva, Dr. A. Siokou, Dr. S. N. Yannopoulos
Foundation for Research and Technology–Hellas
Institute of Chemical Engineering Sciences
(FORTH/ICE–HT), P.O. Box 1414,
GR-26504 Patras, Greece
E-mail: siokou@iceht.forth.gr; sny@iceht.forth.gr
Dr. J. Orava
Department of Materials Science and Metallurgy
University of Cambridge
Pembroke St., CB2 3QZ Cambridge, UK
Dr. J. Orava
WPI-Advanced Institute for Materials Research (WPI-AIMR)
Tohoku University
2-1-1 Katahira, Aoba-ku, Sendai 980-8577, Japan
Dr. M. Pavlista, Prof. T. Wagner
Department of General and Inorganic Chemistry
Faculty of Chemical-Technology
University of Pardubice
Legion´s sq. 565, 53210 Pardubice, Czech Republic
Dr. M. Pavlista, Prof. T. Wagner
Centre for Material Science
Studentska 95, 532 10 Pardubice, Czech Republic

DOI: 10.1002/adfm.201202461

contrary, corresponding efforts in studying materials that exhibit reversible optically-driven structural-transformations within the amorphous phase accompanied by appreciable optical contrast has not been explored. We term this transition "amorphous-to-amorphous transformation" (AAT). The AAT entails mild modifications of structural units after local bonding rearrangements. In practice, AATs have been amply demonstrated in high-pressure studies of bulk glasses (ref. [12] and references therein). We show here that although the AAT is not an actual PC transition, it entails essential differences in the atomic structure of the two distinct meta-stable structures in the amorphous state. The AAT can result in appreciable changes in the optical properties, thus creating new functionalities, which could be exploited in future optical data recording (data storage or holography) and photonic bandgap tuning. In this paper, we attempt to provide a currently lacking, fundamental understanding of the optically-induced AAT in pulsed-laser deposited (PLD) chalcogenide films[13] without, however, demonstrating any of the potential applications.

Experiments on ChGs have shown that a rather small fraction of ≈2% of the all atoms is involved in photo-structural changes such as photodarkening or photobleaching.[14] It should be noted here that since only a small fraction of atoms, ca. 1–2%, are involved is such phenomena, they cannot be considered as real AATs. This relatively low fraction of bonds involved in photo-structural changes entails minor changes of physical-chemical properties and therefore a mild response to an external stimulus. Because in most cases such changes are advantageous for applications, ChGs which exhibit massive photo-induced bond restructuring are of a great interest. It has been recently shown that the fraction of irradiation-affected bonds can be surprisingly high in sulphur-rich binary As-S glasses, i.e., one order of magnitude higher than the corresponding photo-induced reorganized bond fractions reported up to now.[15,16]

Towards exploring new noncrystalline materials with enhanced optically-driven responsiveness and functionality, the key factor to be contemplated relates to the presence of structural motifs in glass that can assist the proliferation of the photo-induced changes. This is achieved when the amorphous structure can provide certain relaxation pathways in order to guide the photo-excited bond to configurations different than the initial one. In this context, nanometer-scale phase-separated amorphous materials, the structure of which contains nanometer-sized environments with similar bonding arrangement, offer possibilities for structural transformations to new meta-stable bonding configurations at low-cost of energy. Solid evidence of nanometer-scale phase separation in arsenic-rich binary As-Se amorphous films, prepared by PLD technique, has been provided in our previous photoemission studies,[17,18] where the nature of the structural motifs presented in the amorphous film was explored in detail. The deposition technique plays a vital role in producing amorphous materials with tailored-made functionalities and the detailed atomistic structure of an as-deposited amorphous film is intimately reflected by the deposition method.[13,14] Thermal evaporation (TE) and magnetron sputtering are the most commonly used deposition techniques. However, a limited number of investigations deal with films prepared by PLD. The PLD is considered as more suitable compared with the classical deposition techniques mentioned above, owing to its advantage of maintaining quite well the composition of the target material in the structure of the films.[19] In addition, PLD films do not suffer from the formation of columnar structures and structural heterogeneities which are associated with irreversible structural transformations and that frequently emerge in oblique-angle TE thin films.[20]

The present study has a twofold objective: (i) employing electronic structure probing technique, namely X-ray photoelectron spectroscopy (XPS), we provide evidence for a reversible switching between two structurally distinct amorphous states. The switching is driven forward and backward by exposure to near-bandgap light and annealing, respectively. The structural changes involved in the AAT are explored in detail. The phenomenon is repeatable in successive cycles of irradiation and annealing for the PLD films while this is not true for the TE films. The AAT does not depend on the order of imposition of the external stimuli, i.e., light and annealing. (ii) Using spectroscopic ellipsometry the two amorphous states are characterized by a large difference in optical contrast exploitable as repeatable change in n of the PLD thin films. The combination of the structural and the optical properties enables us to provide the first, to our knowledge, correlation between the atomic structure and the optical properties of an AAT in ChGs.

2. Results and Discussion

2.1. Structural Details of the AAT in $As_{50}Se_{50}$ Films

Figure 1 shows the XPS As3d and Se3d peaks of as-prepared PLD and TE $As_{50}Se_{50}$ films. Each component of the analyzed spectra is the sum of the 3d5/2 and 3d3/2 contributions and the binding energy (BE) values mentioned hereafter refer to the 3d5/2 peak. The As3d peaks (Figure 1a) are analyzed into three components located at (i) BE ≈ 41.6 ± 0.05 eV (denoted as As^{I}), (ii) BE ≈ 42.1 ± 0.05 eV (denoted as As^{II}), and (iii) weak peaks that appear in the BE range 44–45.5 eV (denoted as As^{III}). The latter refers to arsenic oxides of the form AsO_y,[17,18] which appear due to slight oxidization of the surface in the time interval between film preparation and XPS measurements. Therefore, a mild sputtering took place only after the measurement of the as-prepared films in cycles of the stimulus, causing an unfavorable selective sputtering of Se.[19] A detailed discussion on the justification of the existence of the two distinct local environments, As^{I} and As^{II} in which As atoms participate, can be found in the literature.[15,16] In brief, considering that the structure of As_xSe_{100-x} PLD films with $x > 40$ at% consists mainly of $AsAs_{3-m}Se_m$ pyramidal units, then As^{I} originates from As_4 ($m = 0$) and As_3Se ($m = 1$) pyramids, classified as elemental-like domains. The electronic structure around As atoms in these units is similar and thus the present instrumental resolution does not allow to observe the two discrete components. Accordingly, pyramids As_2Se_2 ($m = 2$) and $AsSe_3$ ($m = 3$) form the stoichiometric-like domains and are considered to be the origin of the As^{II} XPS peak. To ensure that the existence of the above two different nanometer-sized domains is not an artefact of the preparation condition we have investigated several PLD $As_{50}Se_{50}$ films produced from different deposition batches. Analyzing the corresponding As3d XPS peak the fraction of As

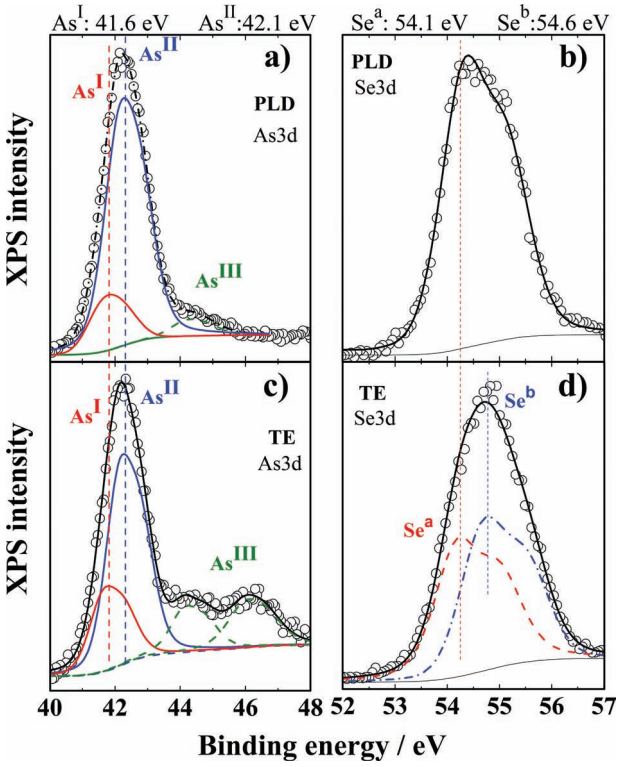

Figure 1. XPS spectra of as-prepared $As_{50}Se_{50}$ thin films. a,b) films deposited by PLD and c,d) films deposited by TE. XPS data show As3d (left panel) and Se3d (right panel) peaks deconvolution after subtracting a Shirley-type background.

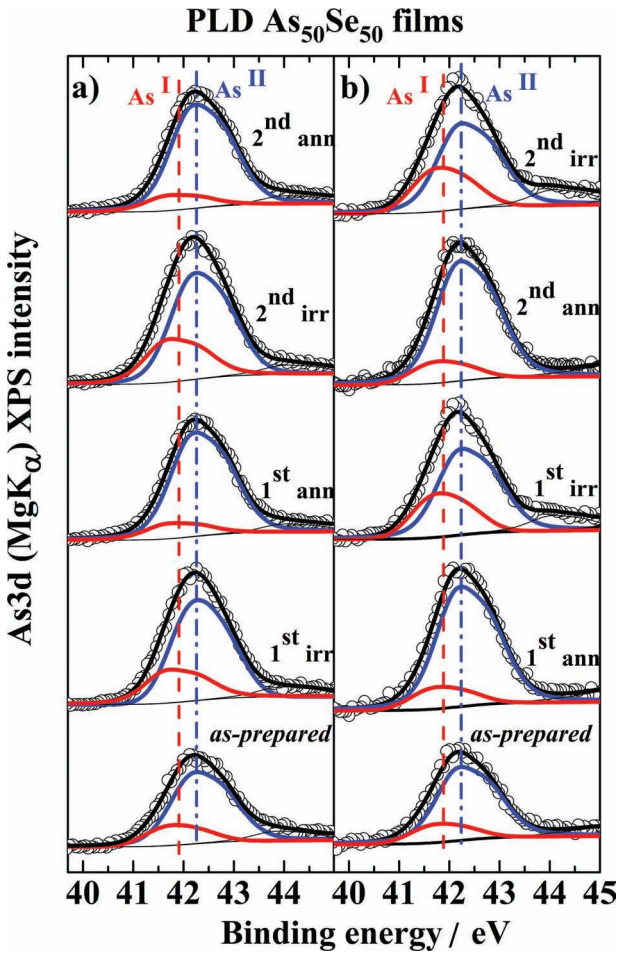

Figure 2. As3d (As^{I} and As^{II}) XPS peak evolution in two cycles. a) As-prepared irradiation → annealing and b) as-prepared annealing → irradiation of PLD $As_{50}Se_{50}$ thin films.

atoms participating in the elemental-like environment (As^{I}) was found to be in range 15–20%.

The Se3d peak of the PLD films (Figure 1b) consists of a doublet peak at BE ≈ 54.2 ± 0.05 eV, which is characteristic of Se atoms bonded to As atoms in the As-Se matrix, denoted as Se^{a} environment. On the contrary, the corresponding Se3d peak of the TE film is analyzed into two components at BE ≈ 54.1 ± 0.05 eV (Se^{a}) and BE ≈ 54.6 ± 0.05 eV (Se^{b}). The former is assigned to Se atoms in As-Se matrix (similar to PDL films), while the latter, which amounts to almost 50% of the total Se3d peak area, originates from Se atoms in Se-rich environments.[15] These results show that the TE films are more heterogeneous compared with the PLD films, exhibiting a bimodal distribution of Se bonding configurations with homonuclear (Se-Se) and heteronuclear (Se-As) bonds. The existence of the extra Se^{b} peak in the TE film is responsible for the enhanced fraction of As^{I} type bonding which amounts to ≈30% of the total peak area, in comparison to the PLD film ≈20%.

Figure 2 shows the XPS As3d spectra of the PLD $As_{50}Se_{50}$ films subjected to recurring annealing and illumination stimuli. Left and right panels in Figure 2 show the changes in XPS signal when the first stimulus imposed is irradiation and annealing, respectively. Two complete irradiation/annealing cycles were performed for each case. The structural changes are quantified in **Figure 3** where the evolution of the $f(As^{I})$ component, defined as the fractional intensity (area) of the peak associated with As^{I}: $f(As^{I}) = I(As^{I})/ [I(As^{I}) + I(As^{II})]$, is shown for the PLD and TE films in Figure 3a,b, respectively. Irrespective of the order to the imposition of annealing and irradiation the fraction of the As^{I} and As^{II} nano-domains varies in a systematic and repeatable way in PLD films (Figure 3a). The As^{I} fraction increases at the expense of the As^{II} fraction with irradiation while it decreases after annealing. No corresponding changes are observed for the Se3d spectra in the course of exposing the structure of the PLD films to annealing and irradiation. The Se3d doublet is always fixed at BE ≈ 54.2 ± 0.05 eV. The reason is that all Se atoms are bonded to As in the as-prepared PLD and neither annealing nor illumination can induce homonuclear Se-Se bonding formation.

Similar experiments were conducted for TE films; the As3d peak evolution (see Supporting Information Figure S1). Illumination induces increase in As^{I} during the first switching cycle, while annealing severely reduces this contribution (Figure 3b). The switching between the two bonding environments for As atoms in TE films does not occur in the second cycle in contrast to the observations of the structural changes in the PLD film. In this second cycle, the As^{I} fraction component approaches that of the as-prepared films and the films structure does not

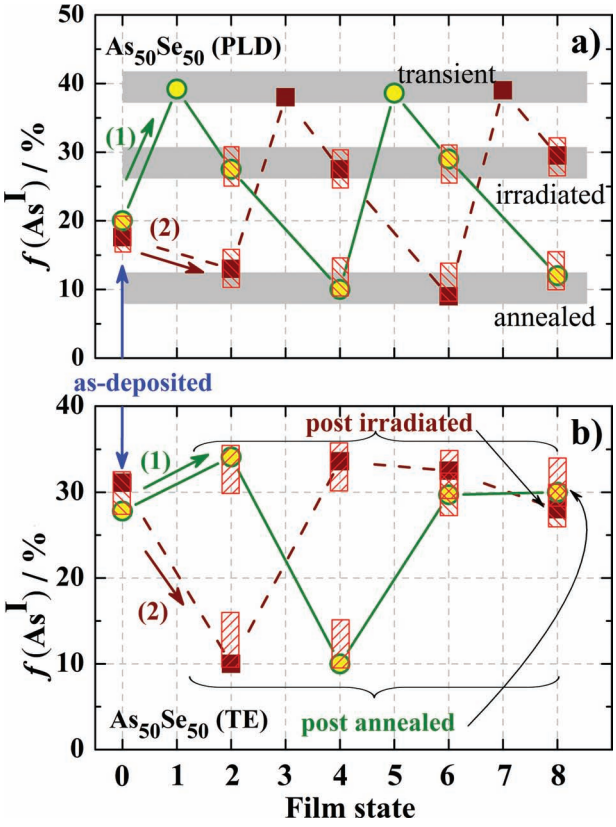

Figure 3. Switching of fraction $f(As^I) = As^I/(As^I + As^{II})$ (%) in films deposited by two different techniques. a) PLD and b) TE $As_{50}Se_{50}$ thing films after alternating external stimuli. The film state values correspond to 0–as-deposited film and 1–8 cycling of irradiation and annealing or vice versa, where route (1)–circles, shows irradiation and route (2)–squares, annealing as first stimuli being applied on as-prepared film. The shaded areas in a) denote three states: transient (laser ON), irradiated and annealedin the upper, middle and lower shaded areas, respectively.

seem to be further amenable to the imposed stimuli. Therefore, in contrast to the effects observed for PLD films where the structure can reversibly switch between two rather well-defined limits, the structure of the TE films, after a complete first cycle of annealing/illumination, attains a configuration which remains stable (inactive) to the imposed stimuli.

In each panel (Figure 3), routes (1) and (2) denote switching cycles where the first stimulus was irradiation and annealing, respectively. In order to ensure the reproducibility of the results, the XPS measurements of the materials under annealing and illumination were conducted several times for both the TE and PLD films. The dashed rectangles enclosing the data points designate the limits within which the values of $f(As^I)$ were estimated by fitting analysis. The data points shown in Figure 3 do not correspond to some average values of the fraction $f(As^I)$ determined from several experiments; they represent the values of $f(As^I)$ for a particular batch of TE and PLD films. The same batch of samples was used for spectroscopic ellipsometry measurements. The irradiation always causes an appreciable increase of $f(As^I)$ (Figure 3a). Irrespective of the film state, either as-prepared or annealed, the magnitude of $f(As^I)$ reaches a rather constant value near 30% indicating the creation of As-As homonuclear bonds and therefore the formation of As_4 and As_3Se structures. It is interesting to note that the films experience also transient photo-structural changes in the course of irradiation as denoted by film states "1" and "5". The fraction $f(As^I)$ amounts to ≈38–40% in the "laser ON" state and falls to the post-irradiation value ≈30% after ceasing irradiation. On the other hand, annealing induces a severe reduction in $f(As^I)$ to a value near 10%, irrespectively of the preannealed state of the film, implying the scission of As-As bonds and the subsequent formation of As_2Se_2 and $AsSe_3$ structural units. Annealing lowers the overall Gibbs energy and tends to smooth out structural defects of the unfavoured structural units As_3Se, As_4 towards the energetically favored ones, As_2Se_2 and $AsSe_3$.

The two well-defined limiting values observed for the PLD films do not occur for the TE films (Figure 3b). While during the first cycle of annealing and irradiation (states "1" and "2") the structural changes would suggest a switching behavior, i.e., annealing and irradiation cause decrease and increase of $f(As^I)$, respectively, the TE film structure ceases to act in response to the external stimuli in subsequent cycles (states "3" and "4"). The fraction of the elemental-like species in the final structure is comparable to that of the as-prepared state. Another point worth noting is that the increase of the $f(As^I)$ caused by irradiation is much smaller than the corresponding decrease caused by annealing, while the "peak-to-valley" changes in the $f(As^I)$ of the PLD films are symmetric around the as-prepared state. This last observation can be rationalized considering that TE films inherited their structure from the gas phase and not from the liquid. The vapor is mainly composed of molecular fragments which contain a larger density of homonuclear bonds which are dictated by the stoichiometry of the material. This enhanced chemical "disorder" resulting from the increased density of defects does not allow irradiation to cause appreciable changes. On the other hand, the annealing of the TE films leads to $f(As^I)$ fractions comparable to those observed in PLD films.

2.2. Correlating Optical Properties and Structure Upon Switching

The significant difference in the population (≈20% as shown in Figure 3) of the structural units, which compose the elemental-like environment in the structure of the amorphous $As_{50}Se_{50}$ PLD films, is expected to have a strong impact on the optical properties. PLD and TE films were subjected to the same scheme of annealing and irradiation, as described in the previous section, and their optical properties were studied using spectroscopic ellipsometry. The optical functions were calculated using three different dispersion models: the Cauchy, the Tauc–Lorentz (TL) and the Cody–Lorentz (CL) models;[21–25] for details see the Supporting Information. **Table 1** compiles the obtained values of the refractive index n at $\lambda = 1500$ nm for two models of analysis (Cauchy and TL), the optical bandgap energy E_g^{opt} (TL), and the Urbach's energy E_U (CL) for the PLD $As_{50}Se_{50}$ thin films.

Figure 4 shows the dispersion of the real part n of the complex refractive index in the spectral range from 900 to 2300 nm calculated using the Cauchy formula, in cycles of the external stimuli, for the PLD films. The refractive index difference (Δn)

Table 1. Values of best-fit models to ellipsometric data calculated by dispersion models. Refractive index n at $\lambda = 1500$ nm (Cauchy: n_C and Tauc-Lorentz: n_{TL}), optical bandgap energy E_g^{opt} calculated by the Tauc–Lorentz model and Urbach's energy E_U calculated by the Cody–Lorentz model in PLD films in two cycles of switching, i.e., irradiation → annealing and annealing → irradiation. The errors in calculated values are $n \pm 0.002$, $E_g^{opt} \pm 0.01$ eV and $E_U \pm 6$ meV.

Cycles of Irr.→Ann.	n_C	n_{TL}	E_g^{opt} [eV]	E_U [meV]	Cycles of Ann.→Irr.	n_C	n_{TL}	E_g^{opt} [eV]	E_U [meV]
As-prepared	2.686	2.687	1.69	100	*As-prepared*	2.688	2.689	1.68	100
Irradiated	2.640	2.648	1.80	88	*Annealed*	2.623	2.626	1.80	83
Annealed	2.605	2.609	1.82	76	*Irradiated*	2.640	2.645	1.76	108
Irradiated	2.642	2.647	1.79	101	*Annealed*	2.602	2.605	1.79	60
Annealed	2.605	2.607	1.82	54	*Irradiated*	2.646	2.652	1.76	91
Irradiated	2.643	2.647	1.86	98	*Annealed*	2.602	2.607	1.78	58
Annealed	2.600	2.611	1.79	73	–	–	–	–	–

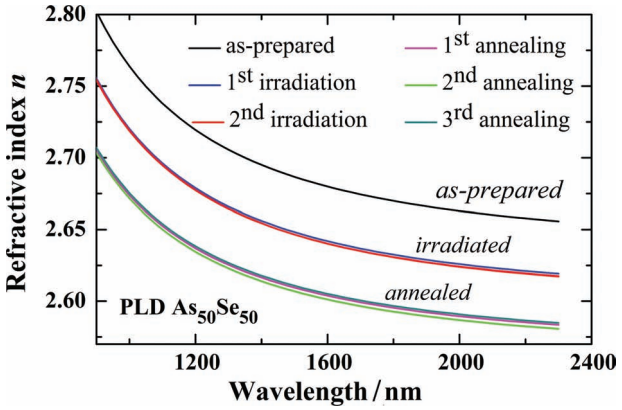

Figure 4. Spectral dependence of refractive index (n) of PLD $As_{50}Se_{50}$ thin films. The data were calculated from best fit using the Cauchy model, and concerns data for both cycles of irradiation and annealing.

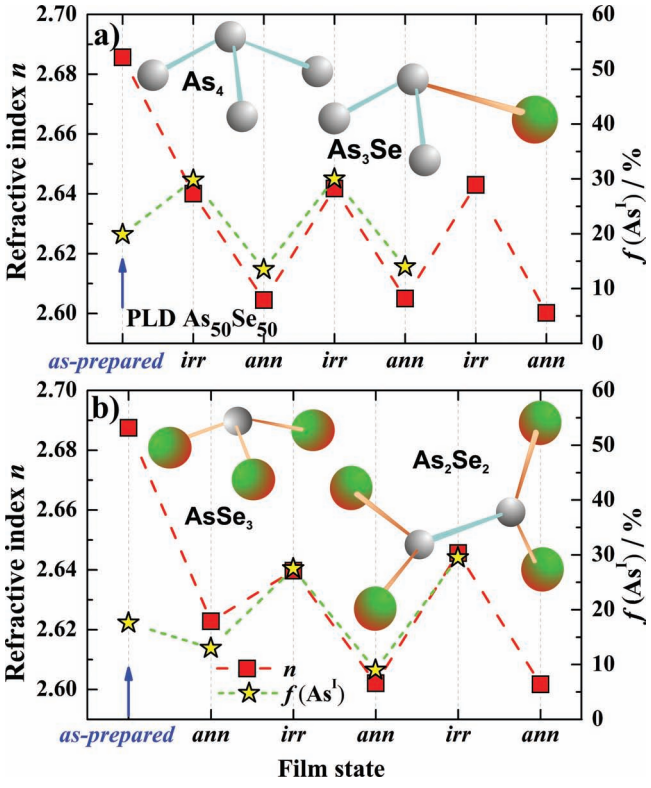

Figure 5. Correlation between changes in refractive index (n) at $\lambda = 1500$ nm (Cauchy) and As3d peak fraction $f(As^I)$. The correlation is depicted for as-prepared $As_{50}Se_{50}$ PLD films after imposing external stimuli in cycle a) irradiation → annealing and b) annealing → irradiation. The insert figures show a schematic of mixed $AsAs_{3-m}Se_m$ (m = 0,1,2,3) structural units which correspond to elemental-like (m = 0,1) and stoichiometric-like (m = 2,3) environments giving rise to a) As^I and b) As^{II} XPS bands, respectively.

between the various film states is practically constant over the whole wavelength range (**Figure 5**). The analysis showed that annealing and irradiation cause negligible changes, of about 0.3% of the initial value, in the thickness of the films and hence volume changes do not affect the accurate determination of n. Systematic decrease in the surface roughness (from 3 to 1 nm), represented by the effective medium approximation layer, with increasing the number of irradiation/annealing cycles was observed. The change in n of PLD films reflects the systematic variation in $f(As^I)$ and switches with the imposition of irradiation and annealing, which is shown for telecommunication wavelength $\lambda = 1500$ nm in the course of applied external stimuli (Figure 5). Irradiation always increases the refractive index to the value $n \approx 2.64$ while annealing decreases its value to $n \approx 2.60$. The increase of n upon irradiation is in agreement with the increase of the fraction of As-As bonds considering that the refractive index of elemental As at $\lambda = 1500$ nm is $n(As) \approx 3.45$.[26] Correspondingly, the decrease of n upon annealing has its origin in the decrease of the fraction of homonuclear As-As bonds and the subsequent restoring of chemical order where heteronuclear As-Se bonding dominates. The results shown in Figure 5 reveal a close correlation between changes in atomic structure (fraction of homonuclear bonds) and optical properties (refractive index) in $As_{50}Se_{50}$ PLD films. Contrary to what is observed for the PLD films the TE thin films did not show any systematic changes in refractive index and $f(As^I)$ (see Supporting Information Figure S2).

The CL model used for the analysis of the ellipsometric data includes the absorption below the optical bandgap E_g^{opt}, thus

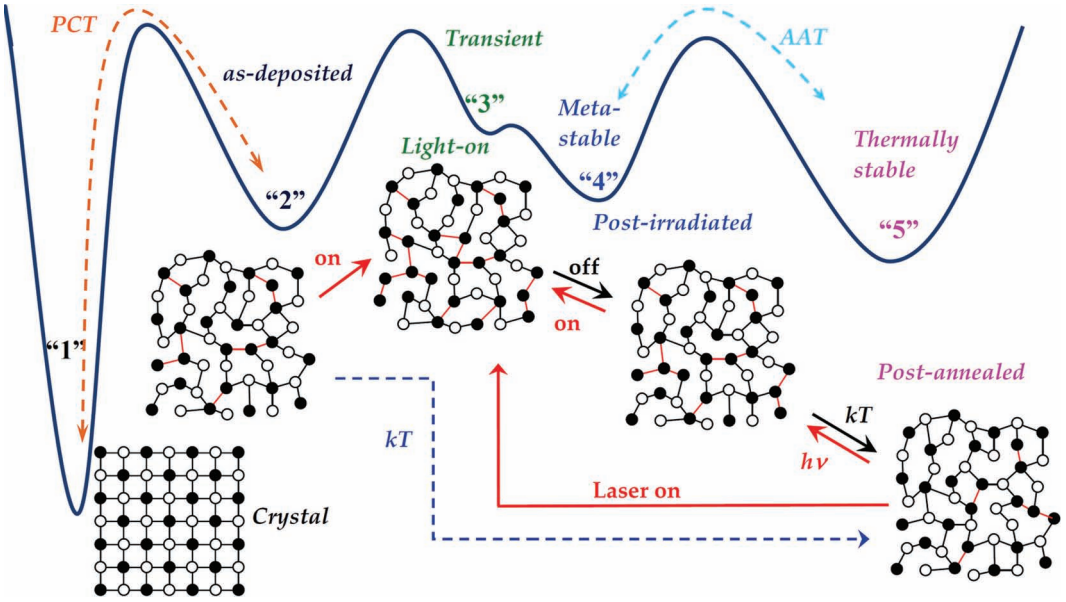

Figure 6. Potential energy landscape representation of the various structural motifs that the $As_{50}Se_{50}$ PLD films can adopt. The deep sharp minimum "1" corresponds to the crystal which has been depicted by an idealized structure (the sketched bonding does not reflect the true molecular crystal structure). The structure of the amorphous as-deposited state "2" is built-up by both As-Se heteronuclear (black lines) and As-As homonuclear (red lines) bonds. In the course of illumination "3", more As-As bonds are formed; the laser excites and transiently traps the structure in a very shallow minimum which allows for relaxation only into the post-irradiated state "4" which is characterized by an As-As bond density larger than state "2" but lower than that of state "3". State "4" is thermally meta-stable; after annealing it relaxes to state "5" which is the amorphous state with the lowest density of homonuclear As-As bonds. Reversible switching in the structure and the optical properties of PLD films occurs between states "4" and "5". State "5" can also be reached from state "2" after annealing.

allowing the calculation of the Urbach's energy E_U (Table 1) The E_U values of the PLD films also exhibit systematic changes following the applied external stimuli and level of chemical "disorder". The origin of the absorption giving the origin of Urbach's edge is still a matter of debate.[27] However, some studies have concluded that the magnitude of E_U reflects the "degree" of disorder in the thin-film structure. The present results show that E_U increases with irradiation (more "disordered" state) and decreases with annealing (less "disordered" state). Disorder here has to be conceived as chemical rather than as topological. It is difficult to assign the change in E_U to any particular bonding behaviour in the studied thin films. It has been shown that the Urbach's edge is mainly governed by the states in the valence band tail.[27] Urbach's edge may appear because the top of the valence band is formed by selenium lone-pairs, which play role in the intermolecular interactions and may therefore influence the disorder.[27] The As-As wrong bonds (defects) lie below the conduction band and are responsible for the weak absorption tail (energies lower than E_U). According to Cody,[28] the E_U depends generally on temperature and disorder. The E_U for the as-prepared TE films was calculated to be within 110–130 meV (±10 meV) depending on the deposition batch.

2.3. Topological View of the Switching Mechanism in Amorphous $As_{50}Se_{50}$ PLD Films: Implications for Applications

The preceding paragraphs on the systematic changes observed for both the short- and medium-range structural order and the optical properties provides solid evidence for a switching phenomenon in amorphous $As_{50}Se_{50}$ thin films prepared by PLD; a property that is lacking in TE amorphous films of the same composition. **Figure 6** shows a schematic of an energy landscape view of the various structural changes described in the preceding sections. In a normal phase-change transition (PCT), starting from the crystal (state "1") one has to provide enough energy to overcome the melting point of the material reaching finally a disordered or glassy state by rapid quenching (>10^9 K/s) (state "2"). Moderate heating is needed to revert the system back to the equilibrium state, i.e., going from "2" to "1". One the other hand, having reached a disordered state "2"–either via melt quenching or by other means such as PLD or TE (the two states can slightly differ structurally)–the present study shows that irradiation and annealing can be used for the controlled, recurring switching between amorphous states with alike, albeit discrete, bonding features. These states are characterized by differences in optical properties. The transient state ("3") corresponds to the structure of the material in the course of irradiation. This can be described by a sufficiently shallow minimum where relaxation to the post-irradiated state "4" is the only possible rather than reverting back to state "2" when ceasing irradiation. The number of As-As homonuclear bonds is the highest of all possible film states as already has been shown in Figure 3. The post-irradiated state "4", reached after ceasing irradiation, is a meta-stable one where the concentration of As-As "wrong" bonds is higher than in the as-deposited "2" state but lower than for the transient state "3". Moderate annealing brings the post-irradiated meta-stable state "4" to a

thermally stable state "5". Irradiation used successively after annealing causes a systematic switching between states "4" and "5", passing temporarily through state "3".

The AAT transition which takes place in $As_{50}Se_{50}$ PLD films could be a more generic phenomenon in non-crystalline media. A prerequisite for this is the existence of a variety of sufficient populations of structural units in the amorphous phase which are amenable to external stimuli, so that the latter can cause reversible transition between them. An advantage of an AAT is that, in non-crystalline media, these structural transformations take place at relatively low-cost of energy. Exploitation to applications, i.e., in optical data storage, depends on the magnitude of the changes in optical properties. The refractive index contrast here is $\Delta n \approx 0.04$, which is almost an order of magnitude lower than the contrast in $Ge_2Sb_2Te_5$ at $\lambda = 780$ nm (CD operating wavelength) and only a factor of two lower for $\lambda = 633$ nm (DVD operating wavelength).[29]

In the course of an AAT, physical properties will change as a result of a cumulative effect of changes in atomic arrangement of certain species; not all atoms (bonds) are expected to participate in the transformation. This implies that switching could be presumably of low-energy consumption in potential devices. The bond energies of heteronuclear bonds As-As and homonuclear bonds As-Se are close to each other 200 and 230 kJ/mol, respectively, making the switching easier.[30] Due to an almost "zero" volume change in the course of an AAT transition, the thin films can be regarded as stress-free during switching contrary to PC-RAM, where the stress during crystallization suppresses the growth rate at low temperatures.[31] In spite of these advantages, the rate of AAT switching, endurance and data retention (amorphous phase drift) which are crucial parameters for potential data storage, remain unknown yet. An extra advantage of an AAT is that a limited number of atoms triggers the switching while in a PC cycle (amorphous ↔ crystal) all atoms must reorganize their positions. The fraction of atoms involved in the AAT determines the responsiveness of the material to illumination (or annealing) which consequently controls the magnitude of the optical contrast between the two structurally different amorphous states.

3. Conclusions

We have provided experimental evidence for the existence of an amorphous-to-amorphous transition in thin $As_{50}Se_{50}$ films prepared by PLD after the imposition of near-bandgap irradiation and annealing. Using XPS and spectroscopic ellipsometry we elucidated the nature of the atomistic changes in this fully reversible switching between two distinct meta-stable states and the corresponding changes in refractive index, respectively.

The switching mechanism is unique for PLD films, whereas no such effect is observed for films of the same composition prepared by thermal evaporation. PLD $As_{50}Se_{50}$ films can be considered as nanostructured surfaces with specialized functionality. The key factor is the existence of nanometer-scale environments with similar bonding arrangement, which facilitate structural transformations to new meta-stable bonding configurations at low-cost of energy. On the contrary, the structure of as-deposited TE films is built-up by structural units that undergo irreversible changes upon irradiation and annealing, lacking the ability to demonstrate switching behavior. In that sense, PLD chalcogenide films become an interesting material for viable applications in photonics, microelectronics and data storage. Exploitation of the diversity of distinct structural states in disordered structures could also provide possibilities for multilever data storage mechanisms.

4. Experimental Section

Thin Film Deposition: Bulk As_4Se_4 glasses were prepared from elements of high purity and after proper homogenization in rocking furnace and melt-quenching were used as rotating targets for the PLD of $As_{50}Se_{50}$ thin films on silicon substrates. A KrF excimer laser operating at $\lambda = 248$ nm with constant output energy of 300 mJ per pulse (pulse duration 30 ns and with repetition rate of 20 Hz) was used for the deposition of the amorphous films at 10^{-4} Pa. The final thickness was determined to be ≈1500 nm on silicon substrate. The composition of the as-deposited films was checked by energy-dispersive X-ray fluorescence. In the case of the As-Se system, the difference between the chemical composition of the target material and the films was found to be within experimental error (±1 at%). Thermally evaporated $As_{50}Se_{50}$ thin films were prepared from the same glassy targets by deposition on Si substrates. Films (≈1050 nm thick) were deposited at pressure 10^{-4} Pa from a resistance-heated silica crucible. The constant deposition rate, measured by the dynamical weighting method was about 1 nm s^{-1}.[32] Energy-dispersive X-ray fluorescence gave also similar film composition as in the case of the PLD films.

X-ray Photoelectron Spectroscopy: The photoemission experiments were carried out in an ultrahigh vacuum system (UHV), which consists of a fast entry specimen assembly, a fast entry chamber, a sample preparation and an analysis chamber with a base pressure lower than 5×10^{-8} Pa. The system is equipped with a hemispherical electron energy analyzer (SPECS LH-10) and a twin anode X-ray gun. For the XPS measurements the un-monochromatized MgKα (1253.6 eV) line was used with constant analyzer pass energy, E_p, 12 and 36 eV for PLD and TE films, respectively. The full width at half maximum (FWHM) of the Se3d XPS peak, of the elemental Se films, is FWHM = 1 eV for $E_p = 12$ eV and FWHM = 1.1 eV for $E_p = 36$ eV. The XPS core level spectra were analyzed with a fitting routine, which can decompose each spectrum into individual mixed Gaussian–Lorentzian peaks after a Shirley background subtraction. Regarding the measurement errors, for the XPS core level peaks and a good signal to noise ratio, errors in peak positions are ± 0.05 eV. The BE scale in XPS measurements is calibrated by assigning the main C1s peak at 284.6 eV.[33] The samples were characterized before and after mild sputtering with argon. All samples were characterized at the as-prepared state as well as after the imposition of the external stimuli, i.e., irradiation and annealing. Annealing took place in the fast entry chamber of the UHV system under N_2 atmosphere (continuous flow) at 150 °C for 90 min. Irradiation took place while the sample was in the UHV using the near-bandgap energy provided by a diode pumped solid state laser operating at $\lambda = 671$ nm (power density ≈300 mW cm^{-2}), for 2 h. The laser was adjusted so that light incidences onto the sample through an optical window of the UHV. The focus of the laser was such that the irradiated area matched the area from which the XPS signal was collected. The external stimuli details concerning the AAT in $As_{50}Se_{50}$ PLD films investigated here were chosen after considering annealing at the highest temperature (150 °C) without the intervention of crystallization. The latter takes place at ≈180 °C for the bulk $As_{50}Se_{50}$ glass.[34] Irradiation times were tested from 30 min to 2 h. Irradiating for 1.5 h was adequate for achieving the maximum alterations in the PLD films' structure.

Spectroscopic Ellipsometry: The optical properties of the thin films were evaluated from the data measured by variable angle spectroscopic ellipsometery (Woollam Inc.) with an automatic rotating analyzer in the spectral range from 0.54 to 4.12 eV, i.e., $\lambda = 300$–2300 nm at three different

angles of incidence 60°, 65°, and 70°. The spectra were measured at 25 nm steps. The ellipsometer was equipped with AutoRetarder, which allows the measurement of the ellipsometric parameter Δ over an interval of 360°. The optical functions were calculated according to following dispersion models. The simple Cauchy formula was used to calculate the dispersion of the refractive index at energies lower than the optical bandgap energy. The Tauc–Lorentz oscillator model (TL) developed by Jellison and Modine was used to describe the complex dielectric function in interband absorption and the transparent regions.[22,23] The TL model adopts the Tauc's formula $\alpha(E) \propto [(E-E_g^{opt})^2/E^2]$ and assumes $\varepsilon_2 = 0$ at energies below E_g^{opt} (Supporting Information Figure S5).[35] The Cody–Lorentz (CL) model developed by Ferlauto et al.[24] is similar to TL in the Lorentz absorption peak and it also defines the E_g^{opt}. However the CL model behaves differently in the absorption onset region as it also includes the absorption below the E_g^{opt} and allows calculation of the Urbach's energy E_U. The annealing and exposure steps were conducted under inert atmosphere (N_2 flow), under the same conditions mentioned above for the XPS measurements. Spectroscopic ellipsometry provides the determination of optical functions of thin films, such as the complex refractive index $N = n + ik$, where n is refractive index and k extinction coefficient. The ellipsometric parameters can be calculated from the complex ratio of the Fresnel's reflection coefficients for two polarized waves, parallel r_p and perpendicular r_s to incidence light direction: $\rho = r_p/r_s = \tan(\Psi)\exp(i\Delta)$. Usually, a model is adopted for the analysis of experimental ellipsometric data. The physical model of the analyzed thin films consisted of three layers: (i) The surface roughness was modeled by using the Bruggeman effective medium approximation (EMA), i.e., the surface layer consisting from the same film material with void density of 50%. (ii) The thin film, the optical function was modeled using either the Cauchy, TL or CL. (iii) The optical properties of the silicon substrate were adopted from the literature[36] and were kept constant during the fitting procedure in order to minimize the number of unknown fitting parameters.

Supporting Information

Supporting Information is available from the Wiley Online Library or from the author.

Acknowledgements

M.K. and J.O. contributed equally to this work. This research was financially supported by the projects CZ.1.07/2.3.00/20.00254 "Research Team for Advanced Non-crystalline Materials" realized by European Social Fund and Ministry of Education, Youth and Sports (MEYS) of the Czech Republic within the Education for Competitiveness Operational Programme for financial support and project LH11101 of MEYS. J.O. acknowledges support from the Engineering and Physical Sciences Research Council (UK). This work was supported by World Premier International Research Center Initiative (WPI), MEXT, Japan. M.K., A. S., and S.N.Y. acknowledge financial support from the Greek State (General Secretariat for Research and Technology-Hellas). We thank Prof A. L. Greer (University of Cambridge, UK) for discussion. This article was modified after online publication. Typographical errors in the affiliation and acknowledgements were corrected.

Received: August 28, 2012
Revised: October 16, 2012
Published online: November 19, 2012

[1] B. J. Eggleton, B. Luther-Davis, K. Richardson, *Nat. Photonics* **2011**, *5*, 141.
[2] J. S. Sanghera, I. D. Aggarwal, *J. Non-Cryst. Solids* **1999**, *256–257*, 6.
[3] J. Ge, Y. Yin, *Angew. Chem. Int. Ed.* **2011**, *50*, 1492.
[4] D. P. Puzzo, A. C. Arsenault, I. Manners, G. A. Ozin, *Angew. Chem. Int. Ed.* **2009**, *48*, 943.
[5] S. R. Ovshinsky, *Phys. Rev. Lett.* **1968**, *21*, 1450.
[6] *Phase Change Materials: Science and Applications* (Eds: S. Raoux, M. Wuttig), Springer, New York **2009**.
[7] J. Orava, A. L. Greer, B. Gholipour, D. W. Hewak, C. E. Smith, *Nat. Mater.* **2012**, *11*, 279.
[8] M. Wuttig, N. Yamada, *Nat. Mater.* **2007**, *6*, 824.
[9] J. Hegedus, S. R. Elliott, *Nat. Mater.* **2008**, *7*, 399.
[10] J. Akola, R. O. Jones, *Phys. Rev. B* **2007**, *76*, 235201.
[11] R. E. Simpson, P. Fons, A. V. Kolobov, T. Fukaya, M. Krbal, T. Yagi, J. Tominaga, *Nat. Nanotechnol.* **2011**, *6*, 501.
[12] M. Vaccari, G. Garbarino, S. N. Yannopoulos, K. S. Andrikopoulos, S. Pascarelli, *J. Chem. Phys.* **2009**, *131*, 224502.
[13] J. Orava, T. Kohoutek, T. Wagner, in *Chalcogenide Glasses* (Eds: J. L. Adam, X. Zhang), Woodhead Publishing (to be published **2013**).
[14] K. Shimakawa, A. V. Kolobov, S. R. Elliott, *Adv. Phys.* **1995**, *44*, 475.
[15] F. Kyriazis, S. N. Yannopoulos, *Appl. Phys. Lett.* **2009**, *94*, 101901.
[16] S. N. Yannopoulos, F. Kyriazis, I. P. Chochliouros, *Opt. Lett.* **2011**, *36*, 534.
[17] A. Siokou, M. Kalyva, S. N. Yannopoulos, M. Frumar, P. Nemec, *J. Phys.: Condens. Matter* **2006**, *18*, 5525.
[18] M. Kalyva, A. Siokou, S. N. Yannopoulos, T. Wagner, M. Krbal, J. Orava, M. Frumar, *J. Appl. Phys.* **2008**, *104*, 043704.
[19] M. Frumar, B. Frumarova, P. Nemec, T. Wagner, J. Jedelsky, M. Hrdlicka, *J. Non-Cryst. Solids* **2006**, *352*, 544.
[20] S. A. Solin, G. N. Papatheodorou, *Phys. Rev. B* **1977**, *15*, 2084.
[21] L. Cauchy, *Bull. Sci. Math.* **1830**, *14*, 9.
[22] G. E. Jellison Jr., F. A. Modine, *Appl. Phys. Lett.* **1996**, *69*, 371.
[23] G. E. Jellison Jr., F. A. Modine, *Appl. Phys. Lett.* **1996**, *69*, 2137.
[24] A. S. Ferlauto, G. M. Ferreira, J. M. Pearce, C. R. Wronski, R. W. Collins, *J. Appl. Phys.* **2002**, *92*, 2424.
[25] J. Orava, J. Sik, T. Wagner, M. Frumar, *J. Appl. Phys.* **2008**, *103*, 083512.
[26] M. I. Zavetova, I. Gregora, *Phys. Status Solidi A* **1977**, *43*, K109.
[27] K. Tanaka, K. Shimakawa, *Amorphous Chalcogenide Semiconductors and Related Materials*, Springer, Heidelberg **2011**.
[28] G. D. Cody, *J. Non-Cryst. Solids.* **1992**, *3*, 141.
[29] S. Raoux, *Annu. Rev. Mater. Res.* **2009**, *39*, 25.
[30] M. Frumar, B. Frumarova, T. Wagner, P. Nemec, in *Photo-Induced Metastability in Amorphous Semiconductors* (Ed. A. V. Kolobov), Wiley, Weinheim **2003**, Ch. 2.
[31] J. Orava, A. L. Greer, B. Gholipour, D. W. Hewak, C. E. Smith, *Appl. Phys. Lett.* **2012**, *101*, 091906.
[32] M. Vlcek, S. Schroeter, J. Cech, T. Wagner, T. Glaser, *J. Non-Cryst. Solids* **2003**, *326*, 515.
[33] D. Briggs, M. P. Seah, *Practical Surface Analysis*, Wiley, New York **1990**.
[34] T. Wagner, S. O. Kasap, *Philos. Mag. B* **1996**, *74*, 667.
[35] J. Tauc, *Amorphous and Liquid Semiconductors*, Plenum, New York **1974**, p. 171.
[36] C. M. Herzinger, B. Johs, W. A. McGahan, J. A. Woollam, *J. Appl. Phys.* **1998**, *83*, 3323.